

Angular Distribution of Neutrons from the $\text{Li}^6(\text{Li}^6, n)\text{C}^{11}$ Reaction at 4.10 MeV*

R. M. BAHNSEN† AND R. T. CARPENTER

Department of Physics and Astronomy, University of Iowa, Iowa City, Iowa

(Received 31 July 1967)

Angular distributions of neutrons from the $\text{Li}^6(\text{Li}^6, n)\text{C}^{11}$ reaction have been measured at 4.1-MeV bombarding energy for all bound levels in C^{11} except the ground state. The 6.39–6.41-MeV doublet was not resolved. The angular distributions, generally, agree in relative magnitude and shape with those from analog states in the mirror reaction $\text{Li}^6(\text{Li}^6, p)\text{B}^{11}$. This result is most easily understood by assuming that both reactions proceed predominately by compound-nucleus formation. The 8.43-MeV level in C^{11} is observed to decay by γ emission even though it is unbound to α -particle emission by 890 keV. This retardation of the α decay cannot be understood as being due to the Coulomb barrier alone.

INTRODUCTION

CHARGED particle reactions induced by bombarding Li^6 with Li^6 have been extensively investigated by many authors.¹ Angular distributions of H^1 , H^2 , H^3 , He^3 , and He^4 have been obtained, in most cases at several energies. No previous work on angular distributions of neutrons from this reaction has appeared.

Although some efforts have been made to explain the angular distributions in terms of direct reactions,^{2,3} they have been generally unsuccessful. Nor are the angular distributions clearly interpretable as arising from a compound nucleus (CN) reaction. Generally speaking, the angular distributions so far obtained are rarely isotropic, with variations in the differential cross sections by factors not exceeding about five being the rule. Symmetry about 90° in the center-of-mass (c.m.) system is required by the identity of the target and beam particles and so can not be used as an argument for a CN mechanism. Analyses in forms of Legendre polynomials^{4,5} usually require orders of six or eight or more. Also, a search has been made for high-energy capture γ rays from C^{12} with negative results,⁶ and an upper limit of $2 \mu\text{b}$ has been placed on the cross section for this reaction. While not precluding a significant CN contribution, this result implies either that the particle-producing reactions from Li^6+Li^6 are predominantly direct, or that the $E1$ radiation widths for states near 30 MeV in C^{12} are unusually small.

Since most of the work done to date has been at bombarding energies below the Coulomb barrier, it

might seem reasonable that the formation of the compound nucleus would be inhibited by the requirement of tunnelling three charges through the barrier. However, it would be difficult to explain on this basis the failure of the $\text{Li}^6(\text{Li}^6, n)\text{C}^{11}$ reaction to proceed by CN formation. It therefore becomes of interest to investigate this reaction and to compare the results to those for the $\text{Li}^6(\text{Li}^6, p)\text{B}^{11}$ reaction involving analogous final states. One expects the former reaction to proceed significantly by CN formation, and correspondence of these angular distributions with those of the latter reaction is strong indication that the two reaction mechanisms are the same.

In the present work angular distributions for the $\text{Li}^6(\text{Li}^6, n)\text{C}^{11}$ reaction have been obtained at a bombarding energy of 4.10 MeV. Neutron energies were measured by a time-of-flight method. The bombarding energy was chosen as a compromise between low yields at lower energies and the need for better time resolution at higher energies. Preliminary accounts of this work⁷ and some of the data acquisition and reduction methods⁸ have already been reported.

EXPERIMENTAL DETAILS

Beams of 4.1-MeV Li^6 ions were obtained from the University of Iowa type CN Van de Graaff accelerator. The ion source and the unique "Y" magnet, which allows mass analysis before the beam is accelerated, have been described in detail elsewhere.⁹ The arrangement of targets and detectors is shown in Fig. 1. The targets consisted of LiF enriched to 96% in Li^6 evaporated onto 0.002-in. thick copper foils. Target thicknesses were approximately 100 keV to the 4.1-MeV Li^6 beam. γ rays were detected by a 3-in. diam \times 2-in. Pilot B scintillator for the angular distribution runs and by a 4×4 in. $\text{NaI}(\text{Tl})$ scintillator for the normalization runs to be described later. In both cases the front face of the scintillator was approximately 1 in. from the

* Work supported in part by the National Science Foundation.

† Present address: Oregon State University, Eugene, Oregon.

¹ T. Lauritsen and F. Ajzenberg-Selove, in *Nuclear Data Sheets*, compiled by K. Way *et al.* (Printing and Publishing Office, National Academy of Sciences—National Research Council, Washington 25, D. C., 1962).

² D. Manesse, M. Coste, C. Lemeille, L. Marquez, and N. Saunier, *Nucl. Phys.* **55**, 433 (1964).

³ S. Takeda and R. Nakasima, in *Proceedings of the Third Conference on Reactions between Complex Nuclei*, edited by A. Gheorco *et al.* (University of California Press, Berkeley, California, 1963).

⁴ George Dudley Ford, Masters thesis, University of Iowa, 1964, SUI Report No. 64-16 (unpublished).

⁵ K. G. Kibler, *Phys. Rev.* **152**, 932 (1966).

⁶ R. R. Carlson and M. J. Throop, *Phys. Rev.* **136**, B529 (1964); M. J. Throop (private communication).

⁷ R. M. Bahnsen, R. T. Carpenter, and R. A. Mendelson, *Bull. Am. Phys. Soc.* **11**, 301 (1966).

⁸ R. M. Bahnsen, R. T. Carpenter, and R. A. Mendelson, *Bull. Am. Phys. Soc.* **11**, 392 (1966).

⁹ D. W. Heikkinen, *Phys. Rev.* **141**, 1007 (1966).

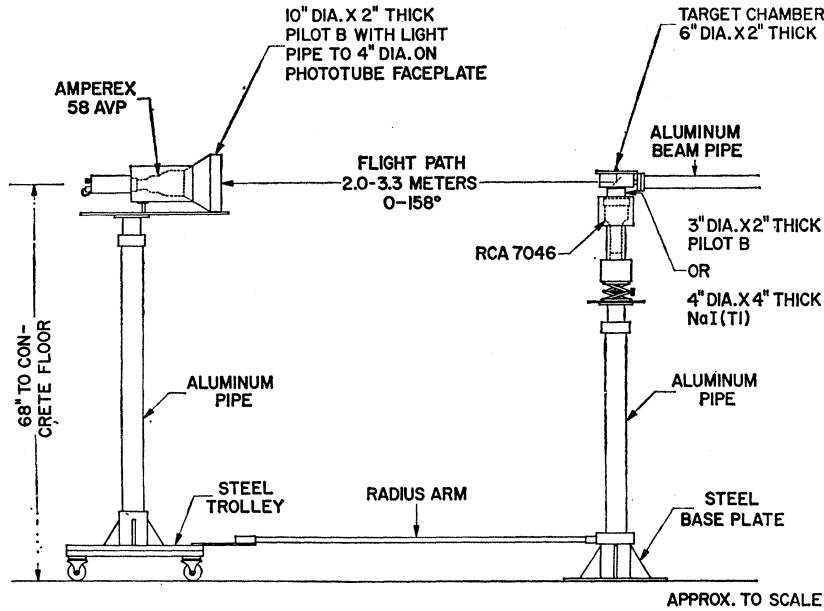


FIG. 1. Experimental geometry.

beam spot. Neutrons were detected by a 10-in.-diam \times 2-in. Pilot B scintillator bonded to a 5-in.-long conical light pipe which had a 4 in. diam at the phototube face. The runs were monitored by a thin ($380\text{-}\mu$) surface-barrier detector fixed at 45° on the side of the beam opposite to that at which the neutron detector was placed. The solid-state detector detected α particles in the 12-16 MeV range which were part of the continuum from the $\text{Li}^6(\text{L}^6, \alpha)2\alpha$ reaction. Singly charged particles in this energy range were not stopped by this detector.

The electronic arrangement used is shown in Fig. 2. Fast pulses from the anode of the photomultiplier tube on the neutron detector triggered a tunnel diode discriminator, the output of which was the start pulse for the time-to-amplitude converter (TAC). The discriminators were of the type discussed by Whetstone and Kounoso.¹⁰ The TAC¹¹ was used on its 125-nsec full scale range. Fast pulses from the γ -ray photomultiplier tube anode were delayed by 110 nsec before triggering a tunnel diode discriminator, the output of

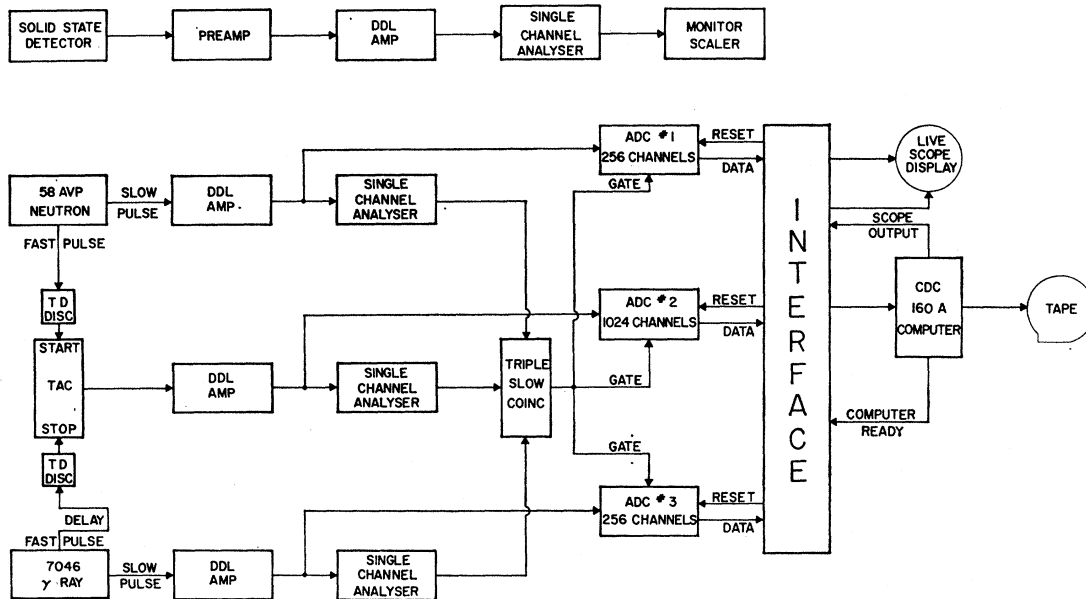


FIG. 2. Block diagram of electronics.

¹⁰ A. Whetstone and S. Kounoso, Rev. Sci. Instr. 33, 423 (1962).

¹¹ Oak Ridge Technical Enterprises Corporation, Model 263.

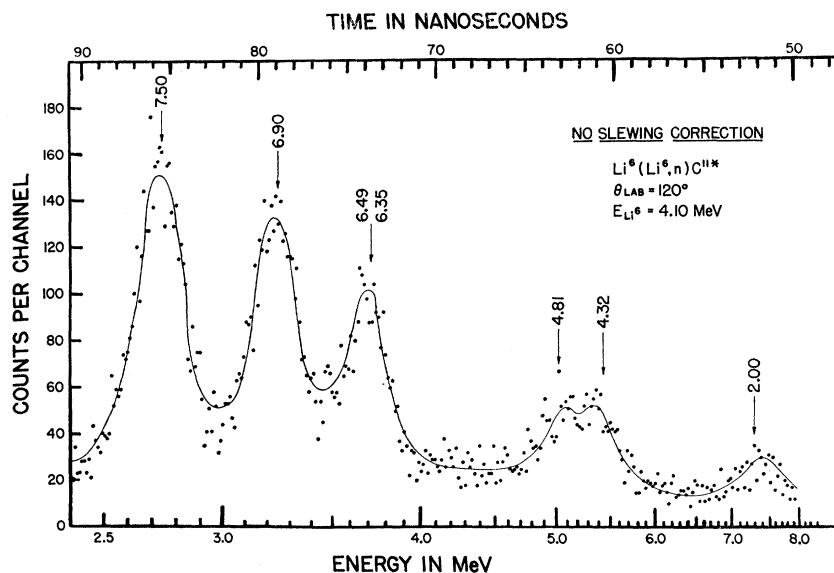


FIG. 3. Time-of-flight spectrum before skewing corrections.

which was used as the stop pulse for the TAC. Slow pulses, obtained from the eleventh dynodes of the phototubes, and the TAC output were amplified by conventional electronics, digitized, and recorded on magnetic tape for off-line analysis. The analog-to-digital converters (ADC's) were gated by a slow coincidence formed on all three analog signals. An upper window on the TAC signal kept the full-scale time pulse, which resulted whenever the TAC received a start signal but no stop signal, from causing excessive dead time in the ADC's.

DATA ACQUISITION

Runs were taken at 0° , 10° , and 30° ; at 10° intervals between 90° and 150° ; and at 158° . Each run required approximately 8 h. The runs were made consecutively over a five-day period. A flight path of 3.3 m was used for the three forward angles in order to obtain adequate resolution with the higher neutron energies, whereas 2.0 m was sufficient for the backward angles. The 158° run was repeated twice to allow a check on target deterioration which was not observed in spite of the rather large beam currents (about $1 \mu\text{A}$) that were used.

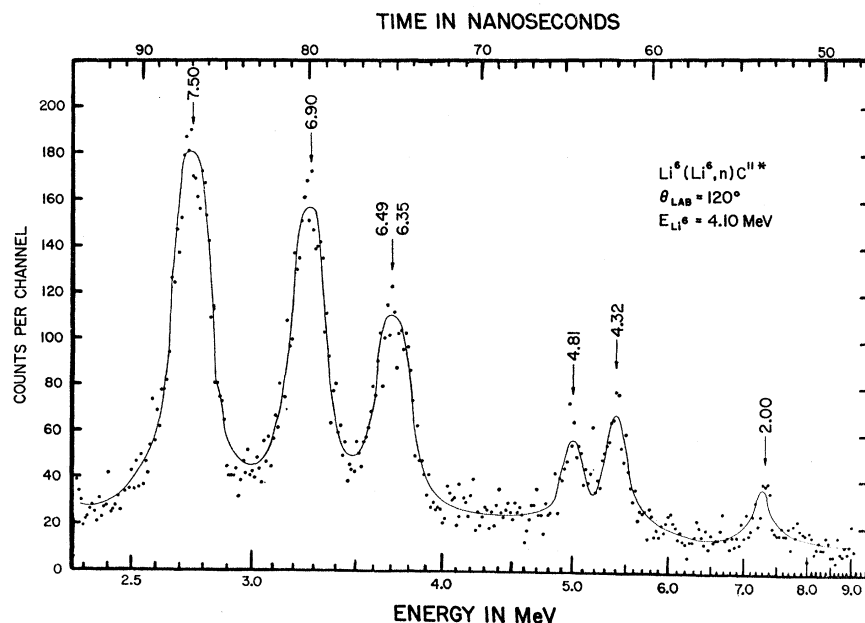


FIG. 4. Time-of-flight spectrum after skewing corrections.

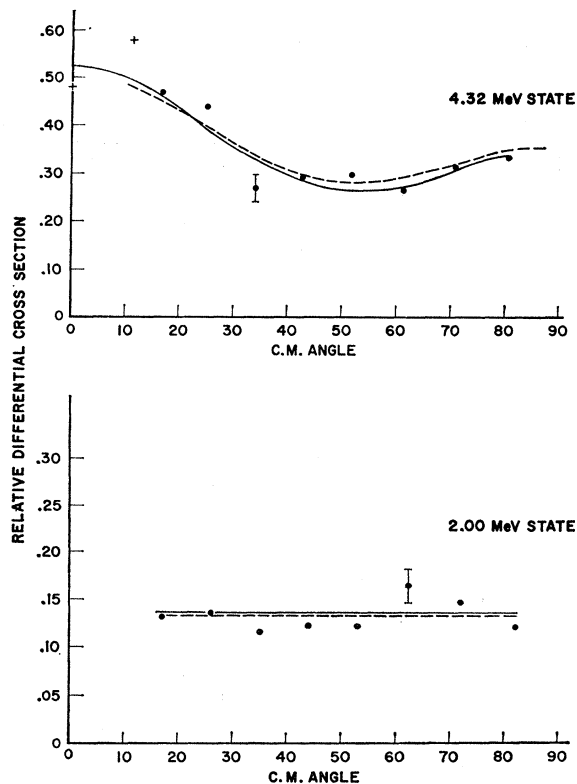


FIG. 5. Angular distributions for the 2.00- and 4.32-MeV states in C^{11} . The solid curve is a least-squares Legendre-polynomial fit. The dashed curve is a similar fit for the mirror states in the $Li^6(Li^6, p)B^{11}$ reaction taken from Ref. 5.

Since the efficiency of the plastic scintillator used to detect γ rays was not known, and since it was desired to normalize the differential yields measured for each state to each other in order to compare with the results for B^{11} , a separate run at 158° was taken using a NaI(Tl) crystal for the γ -ray detector.

DATA REDUCTION

The analysis of the data was performed off line after completion of the experiment. The first step was to improve the time resolution by removing the dependence of each measured time of flight on the pulse heights of the signals involved.⁸ This was possible since both pulse heights were recorded along with the corresponding time of flight. The required correction was determined by examining the prompt peak which resulted from γ - γ coincidences in all reaction products formed and therefore had excellent statistical accuracy. The procedure consisted of scanning the tape to obtain a two-parameter spectrum of pulse height in the γ -ray channel versus time of flight, and thereby to determine the number of channels that should be added or subtracted to the time spectrum for each γ -ray pulse height in order that the time spectrum be independent of γ -ray pulse height. This was then repeated for the neutron

channel. The tapes were then rescanned with a net addition or subtraction performed on each event according to both pulse heights. The improvement obtained in a typical case is illustrated by a comparison of Figs. 3 and 4. The obvious improvement in the spectra corresponds to a decrease in the intrinsic time resolution from 2.9 to 1.2 nsec. The latter figure is still somewhat higher than the optimum value. The main residual source of time resolution broadening results from the use of such large volume scintillators.

Having obtained the spectra, areas under the peaks were determined. In the case of the 4.32-4.81 MeV doublet, a least-squares unpeeling was performed assuming two Gaussian peaks on a constant-slope background. For each state, corrections were made for variations in neutron detection efficiency as a function of neutron energy using standard techniques.¹² Yields to each state were normalized at 158° using the run made with NaI(Tl) as the γ -ray detector. To perform the normalization, the efficiency for detecting a γ ray was taken as

$$\epsilon = \sum_i \epsilon(E_i) f(E_i),$$

where the sum is over all cascade and crossover γ rays that can proceed from the state in question, $\epsilon(E_i)$ is the

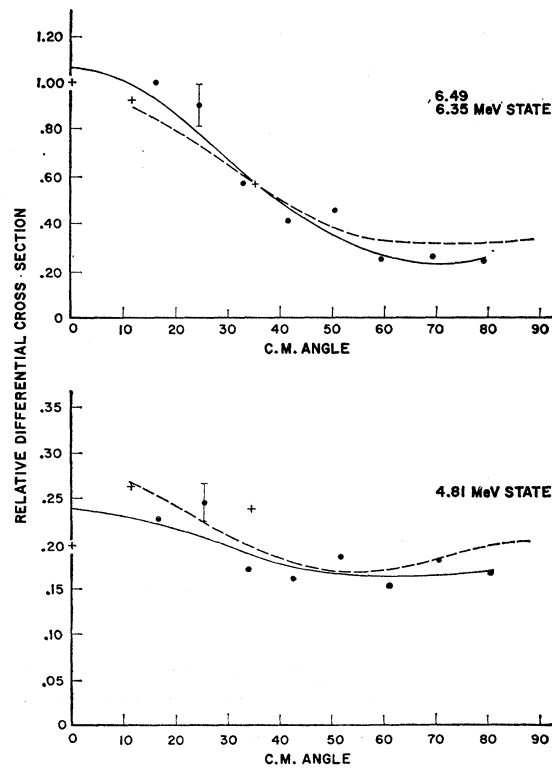


FIG. 6. Angular distribution for the 4.81-MeV state and the group corresponding to the unresolved 6.35- and 6.49-MeV states in C^{11} . See caption for Fig. 4.

¹² G. G. Bonazzola and E. Chiavasa, Nucl. Instr. Methods 27, 41 (1964).

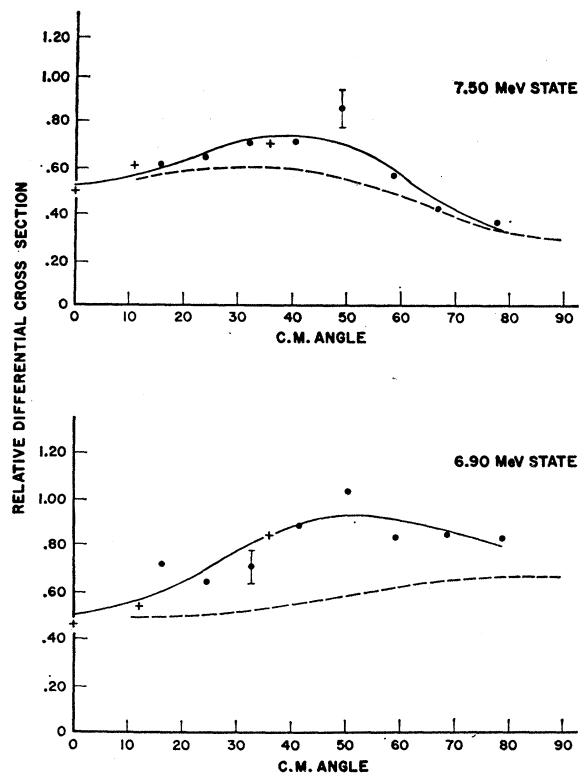


FIG. 7. Angular distributions for the 6.90- and 7.50-MeV states in C^{11} . See caption for Fig. 4.

efficiency for detecting a γ of energy E_i . The efficiencies $\epsilon(E)$ were taken from the Monte Carlo calculations of Miller *et al.*¹³ and the branching ratios $f(E)$ were taken from the work of Olness *et al.*¹⁴

RESULTS AND DISCUSSION

Angular Distributions

Angular distributions in the c.m. system are shown in Figs. 5–7. The scales are arbitrary, but the yields for each state are normalized to each other. The solid curves are Legendre-polynomial fits to the data. The dashed curves in Figs. 5–7 are Legendre-polynomial fits obtained by Kibler⁵ for the $Li^6(Li^6,p)B^{11}$ reaction at 4.0 MeV. Assuming charge independence, the ratio of total cross sections for these two reactions should equal the ratio of momenta of the outgoing particles. Taking this factor into account, the two sets of data have been normalized at the 4.32-MeV state (the 4.46-MeV state in B^{11}). It is seen that there is good agreement between the differential cross sections for the two reactions, except for the 7.50-MeV state (and the 7.99-MeV state in B^{11}) with respect to magnitude and for the 6.90-MeV

state (and the 7.30-MeV state in B^{11}) with respect to both shape and magnitude. A comparison of the total yields to the various states is shown in Table I. This correspondence of differential cross sections is expected *only* in case there are no Coulomb forces acting to break the charge symmetry. However, for the Li^6+Li^6 entrance channel, the Coulomb barrier is approximately 4.8 MeV in the laboratory system, so that the beam energy used was somewhat below the barrier. Thus Coulomb effects are large and, in the case of the direct reaction mode, the probabilities of transferring a He^5 and a Li^5 are expected to be different. Calculations of five-nucleon stripping cross sections including effects of Coulomb distortions are unfortunately not available, so that the nature and magnitude of these differences remain speculative. However, the effect has been observed in the conceptually similar but much simpler case of (d,p) and (d,n) reactions and is well understood.¹⁵ Also, it has been shown¹⁶ that differential cross sections to mirror states in C^{11} and B^{11} do not correspond in the presumably direct $Be^9(He^3,p)$ and $Be^9(He^3,n)$ reactions below the Coulomb barrier. The failure of isospin conservation for lithium-induced reactions below the Coulomb barrier has been discussed by Carlson.¹⁷

However, if the predominant reaction mechanism is compound-nucleus formation, the observed correspondence of the angular distributions is easily explained. In this case, with a bombarding energy of 4.1 MeV, the excitation in C^{12} is over 30 MeV, whereas C^{12} is unbound to protons and neutrons at 15.96 and 18.72 MeV, respectively. Thus, Coulomb effects are negligible in the exit channel and isospin should be conserved in the decay process. Kibler⁵ has estimated on the basis of a simple barrier-penetration calculation that the total compound nucleus cross section for Li^6+Li^6 should be approximately 150 mb at 4 MeV. His measured value for the contribution from proton decay to the bound levels in B^{11} is 25 mb. Assuming the neutron decays contribute equally, taking into account other

TABLE I. Comparison of total neutron yields $Y(n)$ to total proton yields $Y(p)$ obtained in Kibler's paper.^a The ratios in the third column are normalized at the 4.32-MeV state and include factors equal to the ratios of the wave numbers k of the outgoing particles.

C^{11} state (MeV)	B^{11} state (MeV)	$k(p)Y(n)/k(n)Y(p)$
2.00	2.14	0.97 ± 0.10
4.32	4.46	1.00 (normalized)
4.81	5.03	0.95 ± 0.10
6.35/6.49	6.81/6.76	1.01 ± 0.10
6.90	7.30	1.35 ± 0.14
7.50	7.99	1.21 ± 0.12

^a Reference 5.

¹³ L. J. B. Goldfarb, in *Lectures in Theoretical Physics* (The University of Colorado Press, Boulder, Colorado, 1966), Vol. VIII C.

¹⁵ G. V. Din and J. L. Wiel, *Nucl. Phys.* **71**, 641 (1965).

¹⁷ R. R. Carlson and D. W. Heikkinen, *Phys. Letters* **17**, 305 (1965).

¹³ W. F. Miller, S. Reynolds, and W. S. Snow, Argonne National Laboratory Report No. ANL-5902, 1958 (unpublished).

¹⁴ J. W. Olness, E. K. Warburton, D. E. Alburger, and J. A. Beace, *Phys. Rev.* **139**, 512 (1965).

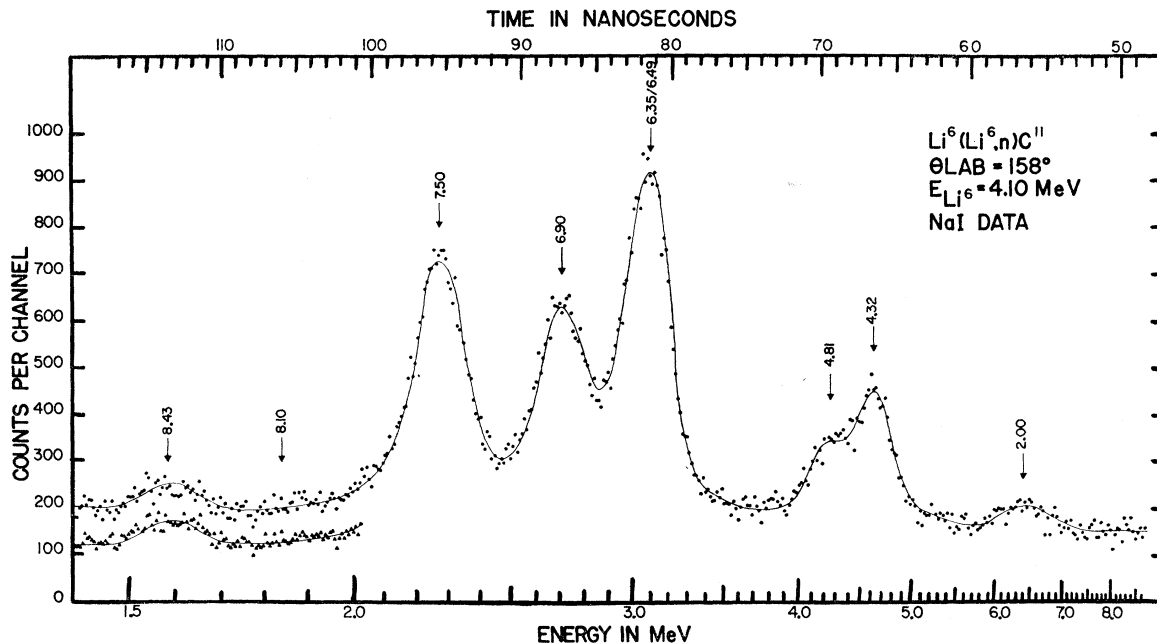


FIG. 8. Time-of-flight spectrum showing the group corresponding to the 8.43-MeV state in C^{11} . A NaI(Tl) crystal was used for the γ -ray detector for this run. The lower curve is data from the same run but scanned with a higher bias level on the γ -ray pulse heights to improve the signal-to-background ratio.

decay modes, errors in the measurements and inadequacies of the approximate calculation, there is no quantitative disagreement in this picture.

8.43-MeV State

In addition to the bound states, n - γ coincidences were observed corresponding to the unbound 8.43-MeV level in C^{11} . This group was most prominently seen in runs using the NaI(Tl) crystal for the γ -ray detector because of its higher efficiency for high-energy γ rays. A time-of-flight spectrum clearly showing the group is shown in Fig. 8. The γ -ray spectrum obtained in coincidence with this group was examined, but the resolution was not adequate to allow determination of branching ratios. However, a γ ray of 8.43 MeV was clearly observed. The group was seen only at forward and backward angles but was generally too weak in the angular-distribution runs to permit a meaningful angular distribution to be determined. In all cases where it

was observed, it appeared in the kinematically correct place for the 8.43-MeV state and was clearly distinguishable from a possible group corresponding to the unbound 8.10-MeV state which was not observed. The mirror level at 8.92 MeV in B^{11} is also known to γ decay.¹⁴ However, this level is unbound to α -particle emission by only 260 keV and the small α width has been attributed to the Coulomb barrier.¹⁴ The 8.43-MeV level is, however, unbound by 890 keV and barrier-penetration calculations show the α -particle emission should clearly predominate over γ decay. The retardation of the α decay suggests that the 8.43-MeV level in C^{11} is a single-particle state of unusual purity for this high an excitation.

ACKNOWLEDGMENTS

The authors would like to thank R. A. Mendelson for help in the construction of some of the electronics, for assistance during the data runs, and for helpful criticism.